Journal of Orthopaedic Translation 24 (2020) 1–11

Contents lists available at ScienceDirect

Journal of Orthopaedic Translation

journal homepage: www.journals.elsevier.com/journal-of-orthopaedic-translation

ORIGINAL ARTICLE

Microsurgical reconstruction affects the outcome in a translational mouse model for Achilles tendon healing

Philipp A. Michel [a,*], Daniel Kronenberg [b], Gertje Neu [c], Josef Stolberg-Stolberg [a], Andre Frank [a], Thomas Pap [d], Martin Langer [a], Michael Fehr [c], Michael J. Raschke [a], Richard Stange [b]

[a] Department of Trauma, Hand- and Reconstructive Surgery, University Hospital Muenster, Muenster, Germany
[b] Department of Regenerative Musculoskeletal Medicine, Institute of Musculoskeletal Medicine, Westfaelische Wilhelms University Muenster, Muenster, Germany
[c] University of Veterinary Medicine Hannover, Foundation, Hannover, Germany
[d] Institute of Musculoskeletal Medicine, Westfaelische Wilhelms University Muenster, Muenster, Germany

ARTICLE INFO

Keywords:
Achilles tendon
Animal model
Heterotopic ossification
Tendon
Tendon healing

SUMMARY

Background: Animal models are one of the first steps in translation of basic science findings to clinical practice. For tendon healing research, transgenic mouse models are important to advance therapeutic strategies. However, the small size of the structures complicates surgical approaches, histological assessment, and biomechanical testing. In addition, available models are not standardized and difficult to compare. How surgery itself affects the healing outcome has not been investigated yet. The focus of the study was to develop a procedure that includes a transection and microsurgical reconstruction of the Achilles tendon but, unlike other models, preserves the sciatic nerve. We wanted to examine how distinct parts of the technique influenced healing.

Methods: For this animal model study, we used 96 wild-type male C57BL/6 mice aged 8–12 weeks. We evaluated different suture techniques and macroscopically confirmed the optimal combination of suture material and technique to minimize tendon gap formation. A key element is the detailed, step-by-step illustration of the surgery. In addition, we assessed histological (Herovici and Alcian blue staining) outcome parameters at 1–16 weeks postoperatively. Microcomputed tomography (micro-CT) was performed to measure the bone volume of heterotopic ossifications (HOs). Biomechanical analyses were carried out using a viscoelastic protocol on the biomechanical testing machine LM1.

Results: A modified 4-strand suture combined with a cerclage for immobilization without transection of the sciatic nerve reliably eliminated gap formation. The maximal dorsal extension of the hindlimb at the upper ankle joint from the equinus position (limited by the immobilization cerclage) increased over time postoperatively (operation: 28.8 ± 2.2°; 1 week: 54 ± 36°; 6 weeks: 80 ± 11.7°; 16 weeks: 96 ± 15.8°, $p > 0.05$). Histological staining revealed a maturation of collagen fibres within 6 weeks, whereas masses of cartilage were visible throughout the healing period. Micro-CT scans detected the development of HOs starting at 4 weeks and further progression at 6 and 16 weeks (bone volume, 4 weeks: 0.07604 ± 0.05286 mm^3; 6 weeks: 0.50682 ± 0.68841 mm^3; 16 weeks: 2.36027 ± 0.85202 mm^3, $p > 0.001$). In-depth micro-CT analysis of the different surgical elements revealed that an injury of the tendon is a key factor for the development of HOs. Immobilization alone does not trigger HOs. Biomechanical properties of repaired tendons were greatly altered and remained inferior 6 weeks after surgery.

Conclusion: With this study, we demonstrated that the microsurgical technique greatly influences the short- and longer-term healing outcome. When the sciatic nerve is preserved, the best surgical reconstruction of the tendon defect is achieved by a 4-strand core suture in combination with a tibiofibular cerclage for postoperative immobilization. The cerclage promotes a gradual increase in the range of motion of the upper ankle joint, comparable with an early mobilization rehabilitation protocol. HO, as a key mechanism for poor tendon healing, is progressive and can be monitored early in the model.

The translational potential of this article: The study enhances the understanding of model dependent factors of healing. The described reconstruction technique provides a reproducible and translational rodent model for future

* Corresponding author. Department of Trauma, Hand- and Reconstructive Surgery, University Hospital Muenster, Waldeyer Str. 1, D-48149, Muenster, Germany. Fax: +49 251 83 56318.
E-mail address: Philipp.Michel@ukmuenster.de (P.A. Michel).

https://doi.org/10.1016/j.jot.2020.04.003
Received 13 December 2019; Received in revised form 17 March 2020; Accepted 8 April 2020
Available online 11 May 2020

Achilles tendon healing research. In combination with transgenic strains, it can be facilitated to advance therapeutic strategies to improve the clinical results of tendon injuries.

Introduction

Tendon injuries are common, have a great impact on quality of life, and pose a notable economic impact on national healthcare systems [1]. The incidence of Achilles tendon ruptures is 28 per 100,000 inhabitants as per a register-based study conducted in Denmark [2]. The overall incidence has been rising in recent decades, based on an increasing incidence of this condition in the older population [3]. Surgical and conservative treatments have several inherent complications, such as rerupture, issues with wound healing, or development of chronic pain [4]. The elastic properties of a healed Achilles tendon are inferior even a long time after rupture [5]. These challenges highlight the need for research and basic animal tendon healing models to study the fundamental physiological mechanisms governing healing [6,7]. Among laboratory animals used to study tendon defects or tenotomy repair, rabbits are the most common (49%), followed by rats (27%) and mice (6%) [8]. Rodents are the most challenging models to use to investigate healing treatments for Achilles, flexor, supraspinatus, and patellar tendons [9]. The small size of the structures complicates surgical approaches, noninvasive imaging techniques, histological assessment, and biomechanical testing. The great advantages of rodent models are low costs, easy handling, and fast generation rates combined with the broad availability of transgenic strains [10].

The mouse models for tendon healing described in the literature can be divided into reconstructive and nonreconstructive techniques. The latter includes excisional, incisional, or complete tendon defects of the Achilles or patellar tendon without repair [11–13]. Only a few authors have used a model with surgical reconstruction of the defect [14,15]. Wong et al. [16,17] found in their studies that a single suture in an uninjured tendon creates an acellular zone surrounding the tied stitch shortly after its insertion. The suture material used for reconstruction has an impact on the healthy tendon and therefore most likely on the healing process.

The only reconstructive model with tenotomy and reconstruction of the Achilles tendon in mice was described by Palmes et al. [18]. The authors used an 8-0 Kirchmayr–Kessler suture combined with a 10-0 circular fine suture. For postoperative immobilization, a 7-0 cerclage was inserted through the tibiofibular fork and placed between the calcaneus and the plantar aponeurosis. In addition, the sciatic nerve was cut to induce denervation of the gastrocnemius muscle. This approach reduced the tension on the reconstructed defect and prevented gap formation and rerupture of the tendon [18]. The authors did not report any signs of heterotopic ossification (HO), although this is a common feature of murine Achilles tendon healing models without surgical reconstruction of the defect [19–22]. In the current literature, the role of HO is not fully resolved. Clinically, HO does not seem to have a major impact after Achilles tendon repair surgery. Although it is observed in up to 28% of the cases after open reconstruction, the rate of HO is comparatively low with current percutaneous techniques [23–25]. A recent study from Howell et al. [26] indicates that HO may be the result of "failed" tendon healing. The authors showed that a divergent differentiation of tenocytes towards cartilage at the expense of tenogenic recruitment leads to persistent fibrosis, which may be one of the key mechanisms underlying poor adult tendon healing [26].

Although the model introduced by Palmes et al. [18] is the only reconstructive technique described in the literature so far, it has several inherent problems:

- The neurotomy of the sciatic nerve is a key part of the model and causes denervation of the gastrocnemius muscle. This may artificially influence the healing process. It is difficult to translate this model into clinical practice. Furthermore, animal testing regulations have been greatly restricted in Europe and the United States in the past decades. The neurotomy of a major nerve to study tendon healing can hardly be justified with current provisions.
- It remains unclear how the different steps of the microsurgical reconstruction itself interfere with the healing process, as the authors did not report any signs of HO with their model.

The focus of the present study was to develop a microsurgical reconstruction technique closer to clinical reality without neurotomy of the sciatic nerve and to assess the macroscopic, histological, and biomechanical outcomes with current methods. Furthermore, we wanted to examine the dependence of the development of HO on different technical aspects of the microsurgical reconstruction.

Methods

Animals

All operational procedures were carried out with permission of the local animal rights protection authorities (approval number: 84-02.04.2015.A310) in accordance with the National Institutes of Health guidelines for the use of laboratory animals. Animal care and treatment were provided in accordance with institutional guidelines. The animals were housed in groups of 2–5 at a constant room temperature of 21°C, at an atmospheric humidity of 65%, and under a 12-h light/dark cycle. They had free access to tap water and standard feed. All operations were performed by a single experienced surgeon during daytime in the laboratory. After the surgical procedure, the animals were returned to their home cages.

Study design

The study was divided into 3 different parts. First, we wanted to confirm the optimal combination of suture material and suture technique for the surgery to minimize the gap formation after 1 week without transection of the sciatic nerve. Second, we wanted to assess macroscopic, histological, and biomechanical parameters for the identified microsurgical technique at 1, 2, 4, 6, and 16 weeks postoperatively. In addition, microcomputed tomography (micro-CT) was performed to detect HOs. Third, we wanted to analyze how the different parts of the operation (e.g., tenotomy or insertion of the suture) itself induced the development of HO.

For all parts of the study, 96 wild-type male C57BL/6 mice aged 8–12 weeks with a body weight ranging from 22 to 28 g were used. The animals were purchased from Jackson Laboratory (Bar Harbor, Maine, USA).

Groups: Part 1

For the first part of the study, the animals were divided into 4 groups (n = 6 per group) with different suturing techniques (as per Kirchmayr–Kessler and Lange techniques). Group size was determined according to tendon healing pilot studies in mice [27,28]. Degradable polydioxanone (PDS II 7-0; Ethicon, Somerville, USA) and Onalon 9-0 (Onatec, Pößneck, Germany) were used as suture materials. In Groups 2–4, a tibiofibular cerclage (Prolene 5-0; Ethicon, Somerville, USA), which is described later in detail, was used for postoperative immobilization (Table 1).

All animals were euthanized 1 week postoperatively as per the standardized institutional protocols. Photographs were taken using a stereomicroscope (Stemi 2000-C + AxioCam ICc 1; Zeiss, Oberkochen,

Table 1
Group design (Part 1) with reference to the technique used, suture material/size, and the immobilization cerclage.

Group	Technique	Suture size/ material	Cerclage
1	Kirchmayr–Kessler	1x PDS 7-0	—
2	Kirchmayr–Kessler + circular fine suture	1x PDS 7-0 + 1x Onalon 9-0	1x Prolene 5-0
3	Lange	1x PDS 7-0 + 1x Onalon 9-0	1x Prolene 5-0
4	Lange	2x PDS 7-0	1x Prolene 5-0

Germany), and the following parameters were documented where applicable: tendon dehiscence, suture material rupture, cerclage dislocation, and wound healing problems.

Groups: Part 2

For the second part of the study, the modified Lange technique was used throughout. The microsurgical technique with 2 PDS 7-0 core sutures and a cerclage showed the least gap formation after 1 week. A total of 6–12 animals per healing time point were euthanized at 1, 2, 4, 6, and 16 weeks postoperatively. All operated hindlimbs were assessed macroscopically for maximum dorsal extension in the upper ankle joint (UAJ) from the equinus position, and photographs were taken to measure the exact range of movement. Subsequently, the Achilles tendons of both hindlimbs were carefully dissected and frozen at −20°C in Phosphate-buffered saline (PBS)-soaked gauze pads for micro-CT analysis and biomechanical testing or fixated with 4% paraformaldehyde for histological analysis [29]. Group size for the different investigations was determined as per previous studies [18,19,30,31].

Groups: Part 3

For the third part of the study, 6 groups (n = 3 per group) were created. We identified 3 core elements of the microsurgical technique:

- Tenotomy
- Tendon core sutures
- Cerclage for postoperative immobilization

For each group, a distinct part of the operation was excluded (Table 2), and the development of HO was assessed 6 weeks postoperatively by micro-CT analysis.

Step-by-step description of the operation technique

The animals were anaesthetized with isoflurane 2.5 vol. % (Forene; AbbVie, Ludwigshafen, Germany) using an inhalation anaesthesia machine (UniVet Porta; Groppler, Deggendorf, Germany) with an oxygen flow of 0.4–0.6 L/min. For analgesia, 4 μg/g body weight of carprofen (Rimadyl; Pfizer, Berlin, Germany) was applied preoperatively and for 3 days after the operation. All surgical procedures were performed under a stereomicroscope using a magnification between 2.5× and 20×. The operation time was measured between the start and end of the anaesthesia.

Table 2
Group design (Part 3) with the partial exclusion of core elements of the microsurgical technique.

Group	Tenotomy	Tendon core suture	Cerclage
1	X		
2	X	x	
3	X		x
4			x
5		x	x
6		x	

Before the start of the surgical procedure, the left hindlimb of the animal was depilated and fixed with a tape on a bench on a prewarmed operation table to achieve a standardized dorsal extension of the UAJ of 30° (Fig. 1A). The skin was washed using a local antiseptic agent (kodan; Schülke, Norderstedt, Germany). A standard size 15-scalpel was used to make a dorsomedial skin incision from the calcaneus to the musculotendinous junction of the Achilles tendon. Extra caution was taken not to injure the medial neurovascular bundle, which runs directly under the skin. After the skin incision, a sterile saline solution was regularly applied to keep the tissue hydrated. To minimize interference with our model, the plantaris tendon was resected (Fig. 1B). The full-thickness tenotomy was then performed approximately 3 mm proximal to the calcaneal insertion using one blade of the microscissors as a cutting surface to protect the surrounding tissue (Fig. 1C and 1D). The next step was the insertion of the tibiofibular cerclage to achieve postoperative immobilization of the UAJ. At first, the M. gastrocnemius with the proximal stub of the Achilles tendon had to be mobilized laterally. The underlying muscular fascia was incised, and the tibiofibular junction was carefully exposed. To ease the preparation process, the fibula was secured with a microsurgical forceps once it was visible (Fig. 1E). The insertion of a Prolene 5-0 suture was facilitated using a standard 22G BD Microlance needle (Becton Dickinson, Heidelberg, Germany), which was slightly bent and used as a suture passer (Fig. 1F and 1G). Once the cerclage was passed ventrally to the fibula, it was ensured that the suture had direct contact with the bone at the lowest point of the junction (Fig. 1H). This was essential to achieve adequate tightening of the cerclage at a later stage. The Achilles tendon was then readapted using the modified Lange technique with 2 independent PDS 7-0 core sutures (4 strands crossing the tenotomy site) (Fig. 1J). For all groups, extra caution had to be taken when handling the tendon stubs with the forceps as the tendon is highly vulnerable to externally applied pressure. The proximal stub can be securely gripped with an atraumatic forceps at the peritendineum between the 2 cords of the tendons. The crossing suture of the Lange technique was then placed 2 mm away from the tenotomy site. The second crossing suture was placed 1 mm away from the tenotomy site (Fig. 1K). The sutures were carefully tightened and cut short (Fig. 1L). After the readaptation of the tendon, the cerclage was placed under the plantar aponeurosis near the calcaneal insertion using a 22G needle as a passer instrument (Fig. 1M). It is essential to stay close to the bone and to have some soft tissue between the calcaneal insertion of the plantar aponeurosis. The cerclage was tightened with the hindlimb taped to the bench until a maximum dorsal extension of 30° of the UAJ was achieved (Fig. 1N). The suture knot was placed close to the tibiofibular junction. To verify the degree of cerclage tightening, the tape was removed, and the maximal joint movement was documented by photographs (Fig. 1O). After rinsing the surgical area, the skin was closed using Prolene 6-0 sutures, and a wound dressing was applied (Fig. 1P).

Histological investigations

The animals were used for histological analysis 1, 2, 4, and 6 weeks after surgery (n = 3–5 per group). Before fixation of the tendons, the location of the tenotomy site was colour marked (Tissue Marking Dyes; BioGnost, Zagreb, Croatia) to facilitate reproducibility in the analysis of the sections. The fixated Achilles tendons (4% paraformaldehyde overnight) were decalcified in 20% EDTA (Carl Roth, Karlsruhe, Germany) for 6 weeks. The tendons were dehydrated using a gradual series of ethanol concentrations (70%, 90%, 96%, and 100%); then, they were saturated with Xylol (J.T.Baker, Center Valley, PA, USA) and embedded vertically in paraffin (McCormick Scientific, Maarn, Netherlands). Using a microtome, serial cross sections were cut at a thickness of 5 μm at the colour-marked tenotomy site.

To qualitatively monitor collagen maturation, Herovici staining was performed (Herovici's Collagen Stain Kit; American MasterTech, Lodi, CA, USA). The staining allows the differentiation of immature collagen

Figure 1. Step-by-step description of the operation technique. Stereomicroscopy photographs: calcaneus, left; gastrocnemius muscle, right. (A–D) A medial incision is made from the calcaneus to the musculotendinous junction, the plantaris tendon is resected, and full-thickness tenotomy is performed. Note the close relationship between medial and lateral vessels directly beneath the Achilles tendon. (E–F) The tibiofibular junction is dissected, the fibula is secured with a forceps, a Prolene 5-0 suture is passed with the help of a slightly bended 22G needle, and the proximal part of the immobilization cerclage is secured temporarily on the operation table. (I–L) Modified 4-strand suture reconstruction (2x PDS 7-0) was performed as per the Lange technique, the tendon is only gripped at the peritendinous sheath to prevent further injury, and sufficient adaption of the tendon stubs is retained. (M–L) The cerclage is passed distally with the help of a 22G needle, a distance of at least 2 mm away from the tip of the calcaneus is ensured, the soft tissue is mobilized medially and laterally, and knotting is accomplished with the appropriate tension to ensure a maximal dorsal extension of 30°, with closure of the skin and application of a wound dressing.

(collagen III, blue) and mature, organized collagen (collagen I, red) [32]. In addition, Alcian blue staining (Alcian blue 8 GX; Carl Roth, Karlsruhe, Germany) was carried out to detect cartilage as a preliminary stage of HO [33].

Micro-CT and bone volume measurement

Micro-CT (SkyScan 1176; Bruker, Kontich, Belgium) was performed on both the left and right hindlimbs starting 4 weeks postoperatively to detect HO (n = 12 per group). Scanning was performed before dissection of the hindlimbs without a filter at a resolution of 8.9 μm. Reconstruction of the data was performed using Nrecon software (Bruker, Kontich, Belgium). The bone volume was measured by segmenting the mineralized from the noncalcified tissue in a defined region of interest between the calcaneus and the musculotendinous junction. This was performed by thresholding all grey values lower than 55 Hounsfield units in the 8-bit image. The measurements were performed using CTan software (Bruker, Kontich, Belgium), which accompanied the micro-CT scanner.

Biomechanical testing

The animals were used for biomechanical testing 2, 4, and 6 weeks after surgery (n = 7–9 per group). The biomechanical tests were performed using the biomechanical testing machine LM1 (TA Instruments, New Castle, USA). Custom-made clamps were used to secure the calcaneus and the proximal part of the Achilles tendon. All tests were performed in a PBS bath at room temperature to prevent desiccation. The viscoelastic testing protocols from Lujan et al. [35] and Dourte et al. [34] were modified to fit the set-up. Before the start of the protocol, the diameter was measured using microscope cameras from 2 different angles. A tendon-specific pretensioning force dependent on the calculated cross-sectional area was applied. After pretensioning, the specimens were subjected to sinusoidal testing at different strain levels (4%, 6%, and 8%) and frequencies (0.01, 0.1, 1, 5, and 10 Hz). A stress relaxation test was performed at the start of every strain level for ten minutes. After the last strain level, the tendons were returned to the pretension force, and a load-to-failure ramp was applied. The analysis of the data was carried out using a custom-designed Matlab (MathWorks, Natick, Massachusetts, USA) protocol. Cross-sectional area (mm^2), static and dynamic E-modulus (N/mm^2), and load to failure (N) were obtained.

Statistical analysis

Statistical calculations were performed using GraphPad Prism 8 (San Diego, CA, USA). Data were analyzed using an ordinary 2-way analysis of variance for repeated measures. For post hoc analysis, Tukey's and Sidak's multiple comparisons tests were used. To examine operation time, the Student t test was used. Statistical significance was set at $p < 0.05$.

Results

Part 1

The modified Lange technique with a 4-strand suture and a cerclage for postoperative immobilization leads to sufficient adaption of the tendon stubs after 1 week

For the first part of the study, a total of 24 animals underwent operations. In Group 1, the sole Kirchmayr–Kessler technique led to a rupture of the suture material and a dehiscence of the tendon stubs in every operated case. Two cases of wound healing problems were detected. The additional application of a cerclage for postoperative immobilization in Group 2 resulted in an approximation of the stubs but left major dehiscence and resulted in a rupture of the sutures in 4 animals. In Group 3, with the modified Lange technique and the cerclage, only 1 case of suture rupture was documented. In Group 4, a sufficient adaption of the stubs was retained in every case, while no suture ruptures were visible (Fig. 2 and Table 3).

Part 2

Partial loosening of the immobilization cerclage led to increasing movement in the UAJ during the healing period

Of the 54 animals in the second part of the study, 5 had a substantial increase in the range of movement of the UAJ after 1 week. This was defined as a maximum dorsal extension of greater than 90°. Dissection of these hindlimbs revealed that the main reason for the increase was a cut-out of the cerclage through or under the plantar aponeurosis. These mice were excluded from further study. All other animals showed no signs of dislocation of the cerclage, and they had macroscopically sufficient healing. Scar tissue around the tenotomy site was visible as soon as 1 week postoperatively. Tendon stubs or sutures were no longer macroscopically visible after 6 weeks (Fig. 3).

The measured maximum dorsal extension in the equinus position showed a significant increasing range of movement during the healing period. One week postoperatively, a value of 54 ± 36° was observed. This increased to 80 ± 11.7° after 6 weeks and to 96 ± 15.8° after 16 weeks (Fig. 4). Dissection revealed that in all cases, the cerclage was still in place at the tibiofibular junction and under the plantar aponeurosis but that it could not fully retain the initial reduction. This partial loosening led to increased movement over the healing period (Fig. 4).

Table 3
Monitored complications per group (Part 1).

Group	Tendon dehiscence	Suture material rupture	Cerclage dislocation	Wound healing problems
1	6	6	—	2
2	4	4	4	0
3	1	1	0	0
4	0	0	0	0

Significant learning curve for the operation time

For the first half of the cohort, the mean operation time was 61.2 ± 14.1 min. The second half of the cohort was operated in 47.9 ± 11 min ($p < 0.001$) (Fig. 4).

Histologic analysis shows a maturation of collagen fibres within 6 weeks

The qualitative analysis by Herovici staining showed predominantly blue dyeability 1 and 2 weeks postoperatively, indicating collagen III production. After 4 weeks, the staining showed shades of red, which further increased after 6 weeks. This suggests a maturation of the collagen fibres to collagen I between 4 and 6 weeks postoperatively (Fig. 5).

Alcian blue staining showed cartilage formation at every time point in the first 6 weeks postoperatively. The largest fractions of Alcian blue–-positive tissue were detected at 2 and 4 weeks with decreasing amounts at 6 weeks (Fig. 5).

The PDS sutures from the initial reconstruction of the tenotomy left 4 holes in the cross section. Between these sutures, a red area marking mature collagen was detectable by Herovici staining after 2 weeks. A serial section of the same tendon with Alcian blue staining revealed a relatively weak signal for cartilage in the corresponding area compared with the rest of the tendon surface (Fig. 6).

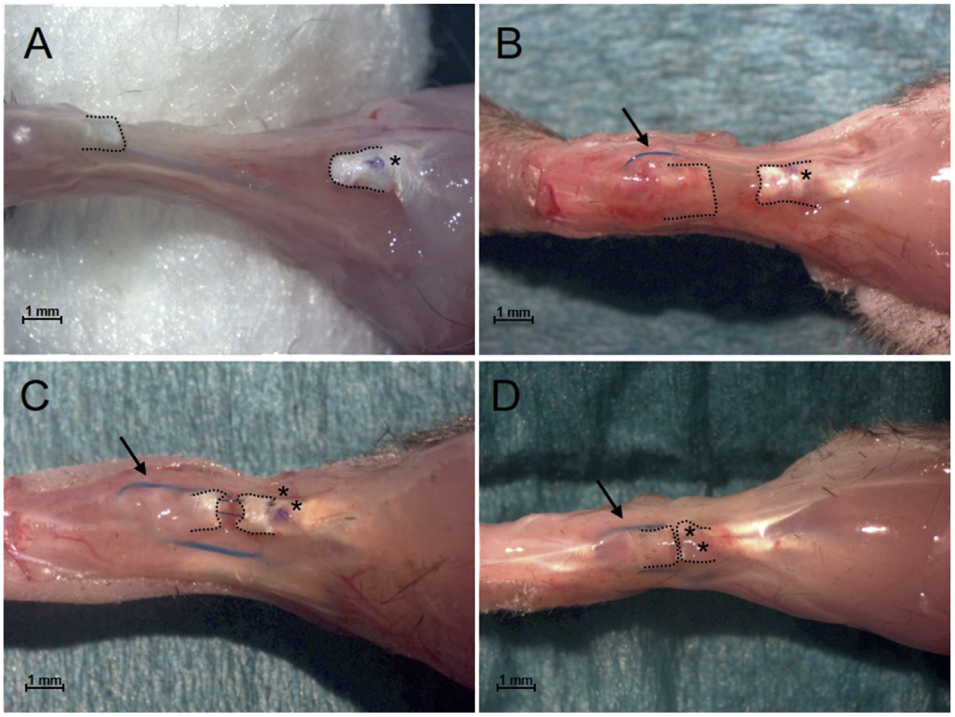

Figure 2. Macroscopic results 1 week after surgery for the different groups (Part 1). Representative stereomicroscopy photographs: calcaneus, left; gastrocnemius muscle, right. The dotted black line marks the tendon stubs, the arrow indicates the position of the cerclage, and * shows the suture knots. (A) Total dehiscence of the Achilles tendon accompanied by suture rupture in a case from Group 1. (B) Although a cerclage for immobilization was applied, the tendon showed a dehiscence, and the sutures were ruptured in a case from Group 2. (C) Partial dehiscence of the tendon with intact suture material in a case from Group 3. (D) Sufficient adaption of the tendon stubs in a case from Group 4.

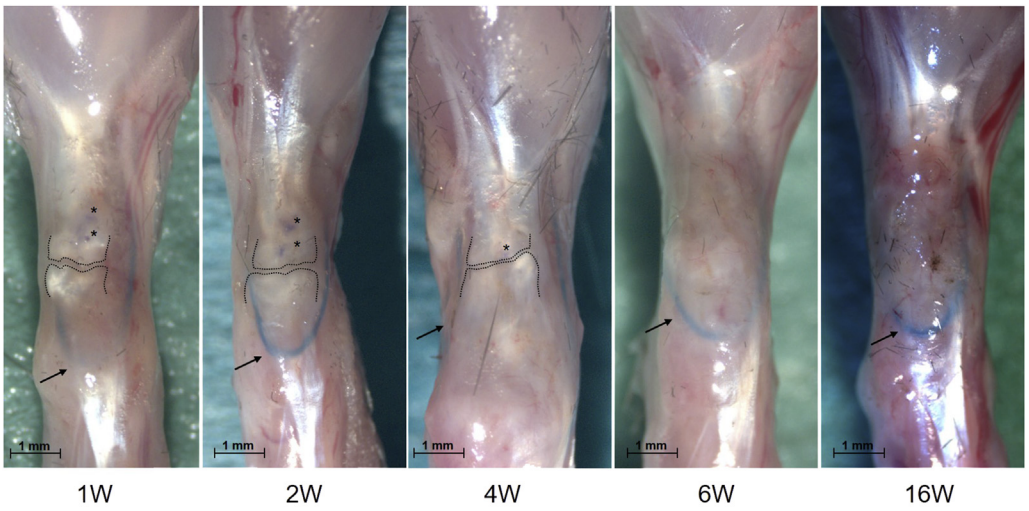

Figure 3. Macroscopic healing results 1–16 weeks (1–16W) after surgery. Representative stereomicroscopy photographs. calcaneus, downwards; gastrocnemius muscle, upwards. The dotted black line marks the tendon stubs, the arrow indicates the position of the cerclage, and * shows the suture knots.

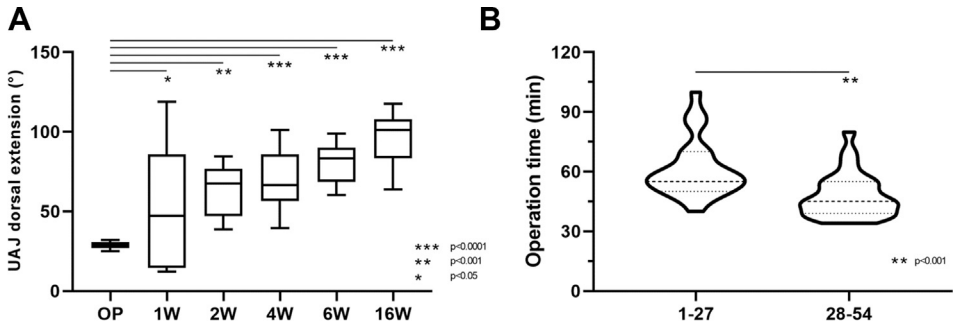

Figure 4. (A) Maximum dorsal extension from the equinus position in the upper ankle joint (UAJ) during the operation (OP) and 1–16 weeks (1–16W) after surgery. A partial loosening of the cerclage facilitates a greater range of motion in the UAJ, mimicking an early mobilization regimen. (B) Mean operation time compared between the first cohort (Animals 1–27) and the second cohort (28–54) shows significant learning.

HOs are detectable after 4 weeks and show a progressive bone volume 16 weeks postoperatively

The micro-CT analysis showed the HO development at 4 weeks postoperatively. A significantly increased ossification bone volume was found after 6 and 16 weeks. The ossifications were located within the tendon between the calcaneus and the musculotendinous junction. Smaller amounts of reactive ossifications were found around the tibiofibular junction and the calcaneus. Within the contralateral tendons, no relevant amounts of HO could be detected (Fig. 7).

Tendon biomechanics are altered in the operated tendons and remain inferior after 6 weeks

The cross-sectional area was significantly increased in the left operated tendons. The load to failure was decreased compared with the nonoperated tendons at all time points. The failure mode was rupture of the tendon within the scar tissue, close to where the tendon had been transected for all specimens. There was no significant difference in the operated tendons between 2, 4, and 6 weeks postoperatively. The static and dynamic E-modulus were significantly reduced in the operated tendons at all time points. There was no detectable recovery for the operated tendons 6 weeks postoperatively (Fig. 8).

Part 3

An injury of the tendon is necessary to trigger HO

For the third part of the study, a total of 18 animals underwent operations. In Groups 1–3 (Fig. 9A–C), which had tenotomies of the Achilles tendon, HO was detected only in the tendon stubs. In Groups 1 and 2 (without a cerclage), a large gap was visible between the HOs, indicating a retraction of the proximal tendon part. With postoperative immobilization with a cerclage (Group 3), the gap was smaller. In Group 4 (cerclage only, no tenotomy or sutures), no HO could be observed within the tendon (Fig. 9D). In Group 5 (cerclage and sutures), a small amount of HO was detected where the sutures were inserted (Fig. 9E). In Group 6 (sutures only), all animals died owing to wound healing problems.

Discussion

Numerous animal models are described in tendon research literature, and all have distinct advantages and disadvantages [36]. The mouse is easy to handle and inexpensive, and there is broad availability of transgenic models. A major drawback is the very small size of the structures. This complicates reconstructive microsurgical techniques and the processing of the specimens with histological and biomechanical methods [37].

The only reconstructive mouse model for Achilles tendon healing in the literature was described by Palmes et al. [18] and includes transection of the sciatic nerve proximal to its bifurcation into the common peroneal nerve and the tibial nerve. This prevents any neurogenic contraction of the gastrocnemius muscle and protects the sutured construct [18]. In contrast, we decided to preserve the nerve to explicitly

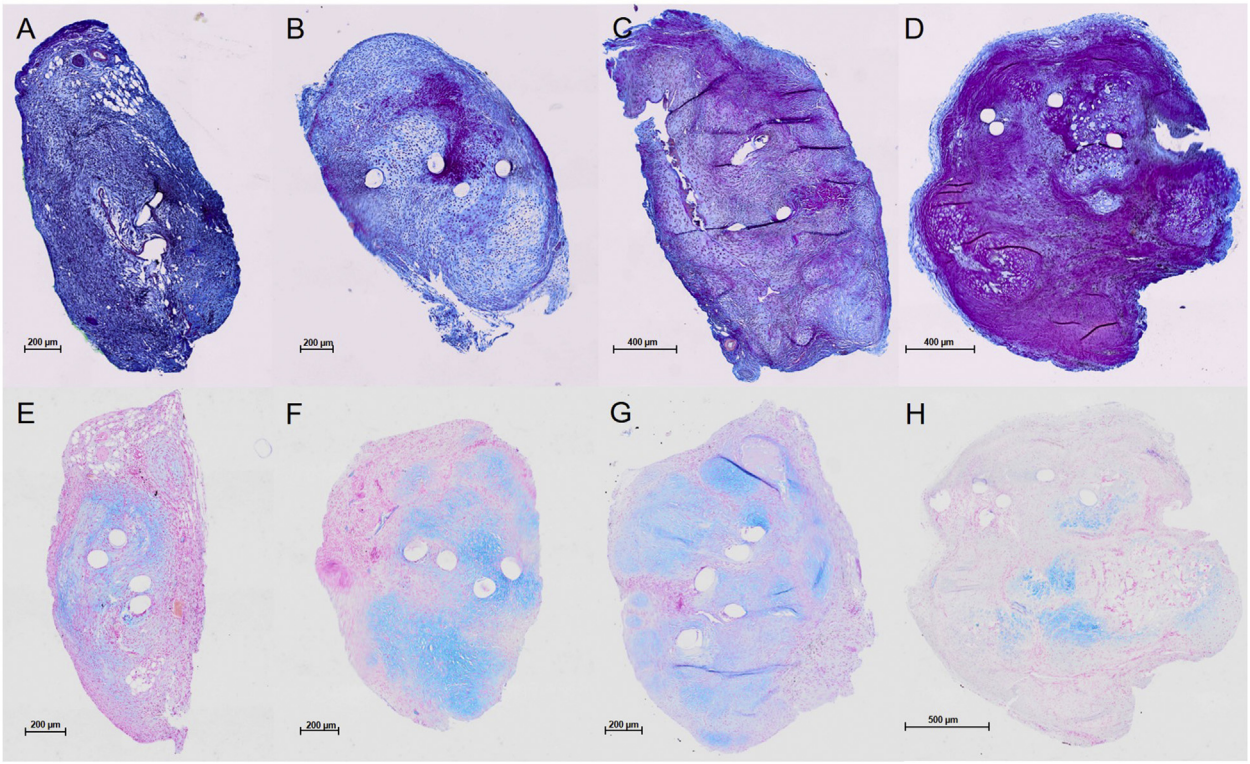

Figure 5. (A–D) Herovici staining of operated Achilles tendons at the tenotomy site 1, 2, 4, and 6 weeks after surgery. (E–H) -Alcian blue -staining of operated Achilles tendons at the tenotomy site 1, 2, 4, and 6 weeks after surgery. Representative cross sections. Round empty spaces match the suture material. (A–D) Blue dye (Herovici staining) indicates younger collagen fibres (collagen III), and red dye indicates mature collagen fibres (collagen I). (C) Maturation of collagen fibres is achieved 4 weeks postoperatively. (D) Maturation of collagen fibres is achieved 6 weeks postoperatively. (E–H) Blue dye (Alcian blue staining) represents chondral cells. Clusters can be detected at every healing stage, and they are less intense 6 weeks after surgery.

expose the sutured tendon to mechanical stress as this is known to greatly interfere with physiological healing processes [38,39]. In addition, this technique is less invasive for the laboratory animal, which eases the approval process with government authorities.

In Part 1 of the study, we found that the modified Lange technique with a 4-strand core suture (PDS 7-0) and a cerclage for postoperative immobilization leads to the most reliable adaption of tendon stubs after 1 week. Thicker suture diameters and a 4-strand suture, compared with the originally described 2-strand and circular fine suture (Dermalon 8-0 and 10-0) combination, were necessary to achieve a stable reconstruction. This is in line with the clinical and biomechanical findings; an increasing number of strands crossing the tenotomy site lead to better biomechanical properties of the construct [40]. In addition, the diameter of the cerclage increased from 7-0 to 5-0. Five animals from the second part of the study had complete dislocation of the cerclage with a cut through the plantaris aponeurosis. The main reason for this was the close proximity to the tip of the calcaneus, with insufficient spare tissue in between them. This complication can successfully be countered by the correct application of the cerclage at approximately 2 mm distal to the calcaneal tip (Fig. 1M). Although we did not directly measure (in vivo) the tension of the reconstructed tendon, the greater suture and cerclage diameter point to an increased tension due to the preservation of the sciatic nerve and the subsequent contractions of the gastrocnemius muscle.

In Part 2 of the study, we observed a partial loosening of the cerclage, which led to an increased amount of dorsal extension in the UAJ. A gain of approximately 10–15° per week was documented, resulting in an almost neutral joint position (90° dorsal extension from the equinus position) 6 weeks postoperatively. This mirrors a gradual increase in the range of movement as would be found in an aftercare protocol. It can be compared with early mobilization rehabilitation regimens used in the clinic after Achilles tendon ruptures, which have led to better functional results [41,42].

The histological analysis shows a maturation of collagen fibres from collagen III to collagen I between 4 and 6 weeks postoperatively. Like other authors, we could detect cartilage formation starting 1 week postoperatively. These cartilage masses mineralize after 4–6 weeks, most likely through enchondral ossification [43]. Interestingly, we found hints that local strain variances influence the pace of collagen maturation and distribution of cartilage. Several serial cross sections showed red-stained areas 2 weeks after surgery where 2 sutures were located close together. The corresponding area was weakly stained for Alcian blue. As the distance between sutures is hardly a controllable surgical parameter, this finding was not consistent in all analyzed sections. Other authors have found that mechanical tension influences cell differentiation, possibly towards an osteogenic phenotype [44,45]. The exact underlying mechanisms are not within the scope of the study design and must be resolved in further studies [46].

Corresponding to these findings is the detection of HO after 4 weeks in the micro-CT scans. Bone volume significantly increased after 6 weeks and 16 weeks postoperatively. Although Palmes et al. [18] did not comment on the development of HO, they described “occasional transition into fibrocartilage that appeared as islands dispersed between the fibre bundles” 16 weeks postoperatively. An explanation for these differences might be the reduced tensile loading because of the missing contraction of the gastrocnemius muscle. Ackerman et al. [47] did not report the appearance of HO with their model 28 days postoperatively. They used a similar principle of reduced tension with a double tenotomy of the flexor digitorum longus tendon. By transecting the tendon proximally to the reconstruction, the influence of the muscle contraction was eliminated [47]. Although this is the same concept, it remains unclear whether HO generally occurs during flexor tendon healing. In addition to Achilles tendon healing, HO has been reported in mouse patellar tendon healing [48]. Similarly, O'Brien et al. [20] have shown that needle injury to the Achilles tendon without any reconstruction or immobilization

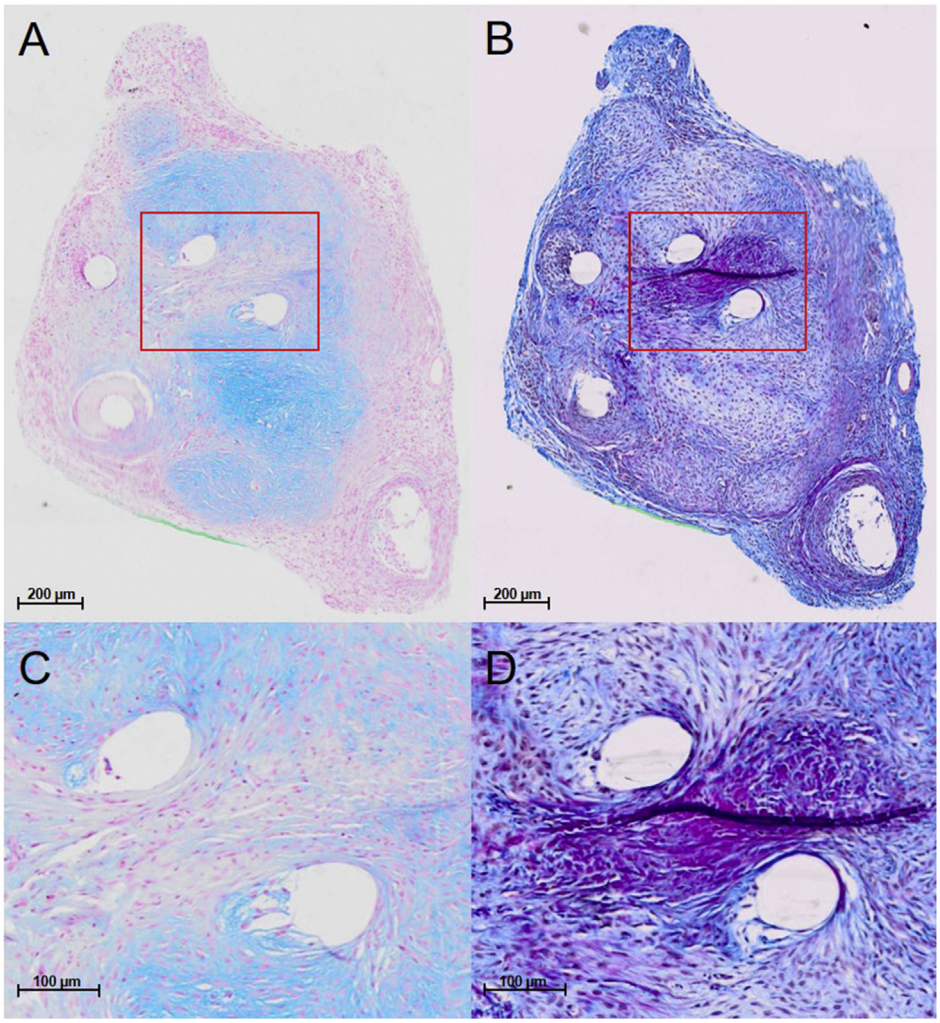

Figure 6. (A and C) Alcian blue staining of an operated Achilles tendon at the tenotomy site 2 weeks after surgery. (B and D) Herovici staining of an operated Achilles tendon at the tenotomy site 2 weeks after surgery. (A and B) Representative cross sections. (C and D) Magnifications of the area of interest. Round empty spaces match the suture material. Local strain variances seem to influence the pace of collagen maturation and distribution of chondral cells.

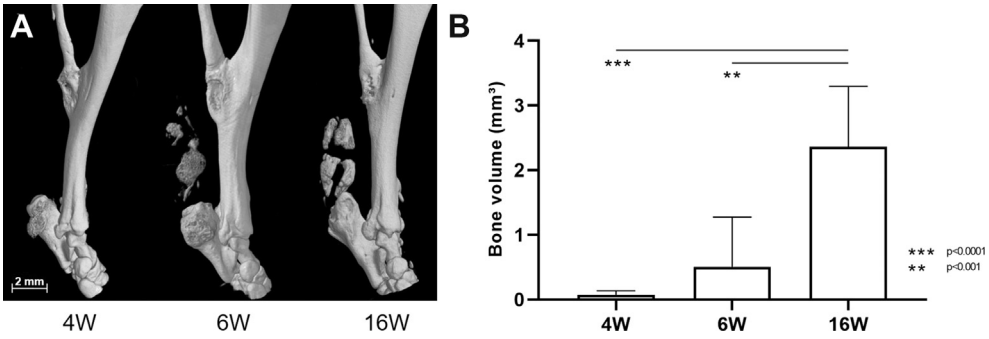

Figure 7. (A) Micro-CT scans of operated hindlimbs 4–16 weeks (4–16W) after surgery. (B) Measured bone volume in the region of interest between the calcaneus and musculotendinous junction. Heterotopic ossifications (HOs) can be detected starting at 4 weeks after surgery and show progression over time. CT = computed tomography.

leads to massive HO after 20 weeks. Zhang et al. [19] found ectopic cartilaginous mass formation 4 weeks after surgery in a complete Achilles tendon transection model without reconstruction or immobilization. Injury-induced ectopic tendon mineralization is progressive; they reported a 2.5-fold increase in bone volume between 10 and 25 weeks [19]. We found the same trend, but the onset was earlier, and the progression seemed to be faster in our model than in theirs. A possible explanation for this is the influence of the suture material, which might lead to regional differences in tension within the tendon. The development of HO in our model is in line with the concept of persistent fibrosis mentioned by Howell et al. [26]. Accordingly, we found HO in our model in the remaining tendon stubs. As the tendon was reconstructed without a gap, the HOs were distributed from the calcaneus to the musculotendinous junction. From our data and from the data presented in the literature on

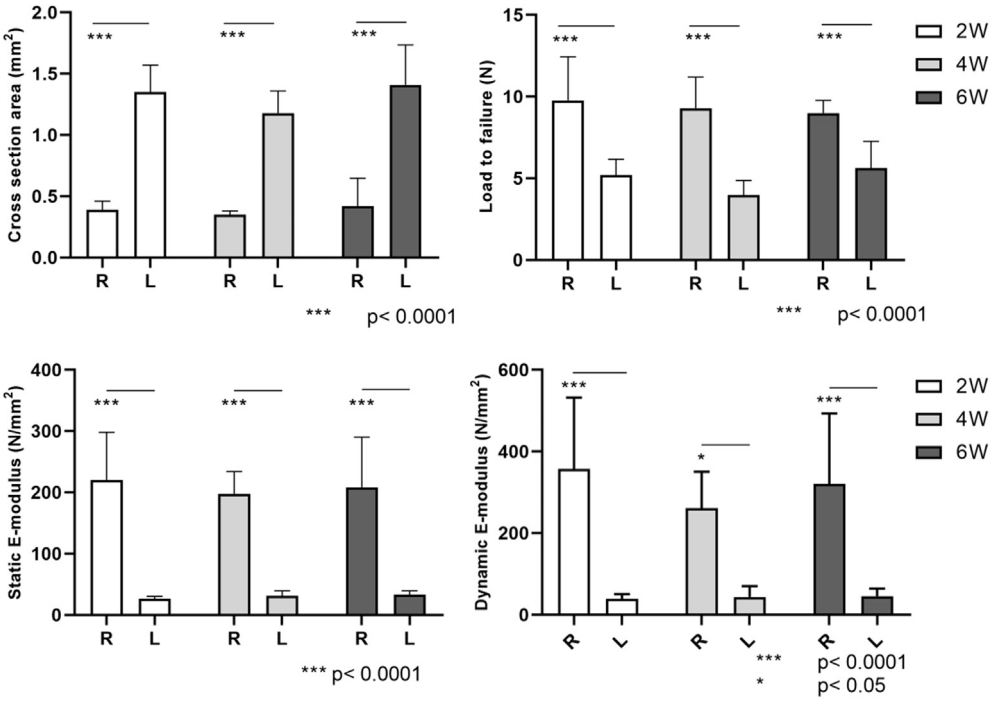

Figure 8. Biomechanical properties of right (unoperated) and left (operated) Achilles tendons 2–6 weeks (2W–6W) after surgery. W = weeks.

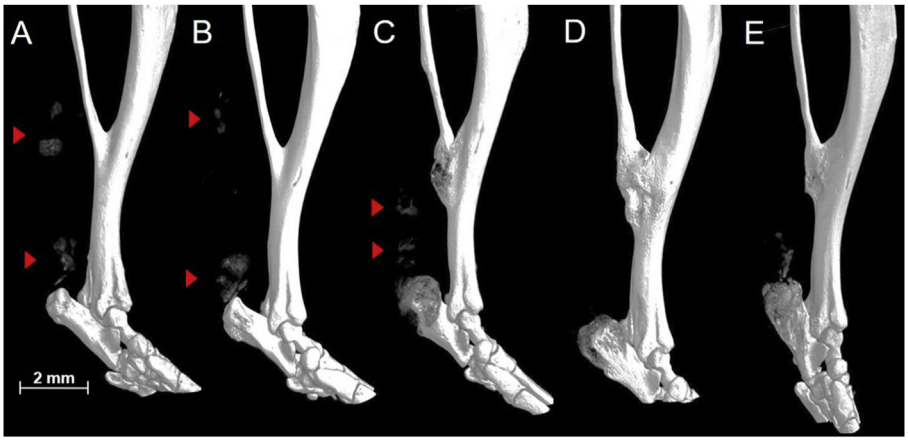

Figure 9. Representative micro-CT images of operated hindlimbs (Part 3). (A) Tenotomy of the Achilles tendon without reconstruction of the defect leads to ossification of the tendon stubs (red arrows) with a gap (Groups 1 and 2). (B) Tenotomy of the Achilles tendon with reconstruction of the defect leads to ossification of the tendon stubs (red arrows) with a gap (Groups 1 and 2). (C) Tenotomy and cerclage decreased the gap between the ossified stubs (Group 3). (D) No ossifications were detected in the group with cerclage alone (without tenotomy and reconstruction, Group 4). (E) Cerclage and reconstruction without tenotomy lead to the development of moderate ossifications (Group 5). No micro-CT images were available for Group 6 (see text).

HO, tensile loading seems to further enhance the development of HO in Achilles tendon healing models [49].

The biomechanical properties of the operated tendons are greatly altered and remain inferior 6 weeks after surgery with our reconstruction model. Zhang et al. [19] made similar observations with their model. They found a dramatically reduced dynamic modulus after 10 and 25 weeks, as well as reduced maximum stress [19]. O'Brien et al. [20] did not detect significant differences in the tangential stiffness and failure load between control, uninjured, and injured tendons at the time points used in their study. They did not test for the dynamic modulus [20]. Although it is difficult to compare these studies owing to different surgical models, postoperative time points, protocols, and infrastructure for biomechanical testing, the dynamic modulus seems to be greatly affected by the HO and drops to approximately 15% compared with that of the control group. As the HOs are progressive, no recovery of biomechanical properties can be observed.

Summarizing the structural and biomechanical results, we could demonstrate that the microsurgical reconstruction of the tendon leads to an inferior “tendon scar”, which mirrors the features of poor human tendon healing [50].

In Part 3 of the study, we showed that an injury to the tendon seems to be necessary to induce the formation of HO. A tenotomy of the tendon without sufficient reconstruction (Groups 1–3) led to an ossification of the tendon stubs. This finding is in line with the aforementioned studies from O'Brien et al. [20] and Zhang et al. [19]. Interestingly, the application of cerclage alone in Group 4 did not lead to the development of HO in the tendon. In Group 5 (sutures + cerclage), a small amount of ossification was detected compared with that in the standard technique. Microinjury through the needle seems to be a sufficient trigger for HO. The wound healing problems in Group 6 can be explained by the friction of the suture material under the skin, which is largely increased without immobilization. All animals had to be euthanized due prematurely.

The study has several limitations. First, the results of animal models must be interpreted with care when transferring the findings to clinical practice. The anatomy and gait of mice are different. The maximum movement in the UAJ in mice is greater than that in humans (plantar flexion/dorsal extension mice: 90/0/70° vs. humans: 45/0/30°). The operation time was quite long (~50 min per animal for the second

cohort), especially in comparison with the operation time in non-reconstructive models. Although a significant learning curve could be observed, it reflected the difficulty of the microsurgical operations steps and the fastidious application of the cerclage and the 4-strand suture.

In conclusion, we demonstrated that the microsurgical technique had a great impact on the outcome in a translational mouse model for Achilles tendon healing. When the sciatic nerve is preserved, the best surgical reconstruction of the tendon defect is achieved by a 4-strand core suture in combination with a tibiofibular cerclage for postoperative immobilization. The cerclage promotes a gradual increase in the range of motion of the UAJ, comparable with an early mobilization rehabilitation protocol. HO, which is a key mechanism for poor tendon healing, is progressive and can be monitored early within the model. Immobilization alone does not lead to the development of ossifications within the tendon. The biomechanical properties of operated tendons are altered and do not recover over time.

The study enhances the understanding of model-dependent factors of healing. The described reconstruction technique provides a reproducible and translational rodent model for future Achilles tendon healing research. In combination with transgenic strains, it can be facilitated to advance therapeutic strategies to improve the clinical results of tendon injuries.

Funding

This research did not receive any specific additional grant from funding agencies in the public, commercial, or not-for-profit sectors, and no material support of any kind was received.

Conflict of Interest

The authors have no conflicts of interest to disclose in relation to this article.

Author contributions

P.A.M. performed the operations and biomechanical testing and wrote the manuscript. J.S.-S. and G.N. assisted during the operations and performed animal care. D.K. and G.N. conducted the histological investigations and microcomputed tomography analysis. A.F. analyzed the biomechanical data. All authors made substantial contributions to the research design, the interpretation of data, and the critical revision of the article. All authors have read and approved the final submitted manuscript.

Acknowledgements

This study was supported by the EXC 1003 (Cluster of Excellence 1003) and Cells in Motion (CiM). The authors thank S. Niehues and I. Leifert for technical assistance. The authors thank R. Gronewold for the help with animal care. The authors thank Marcus Müller for assistance building the biomechanical test set-up.

Appendix A. Supplementary data

Supplementary data to this article can be found online at https://doi.org/10.1016/j.jot.2020.04.003.

References

[1] Nourissat G, Berenbaum F, Duprez D. Tendon injury: from biology to tendon repair. Nat Rev Rheumatol 2015;11(4):223–33 [English].
[2] Ganestam A, Kallemose T, Troelsen A, Barfod KW. Increasing incidence of acute Achilles tendon rupture and a noticeable decline in surgical treatment from 1994 to 2013. A nationwide registry study of 33,160 patients. Knee Surg Sports Traumatol Arthrosc 2016;24(12):3730–7.
[3] Lantto I, Heikkinen J, Flinkkila T, Ohtonen P, Leppilahti J. Epidemiology of Achilles tendon ruptures: increasing incidence over a 33-year period. Scand J Med Sci Sports 2015;25(1):e133–8.
[4] Yang X, Meng H, Quan Q, Peng J, Lu S, Wang A. Management of acute Achilles tendon ruptures: a review. Bone Joint Res 2018;7(10):561–9.
[5] Frankewycz B, Penz A, Weber J, da Silva NP, Freimoser F, Bell R, et al. Achilles tendon elastic properties remain decreased in long term after rupture. Knee Surg Sports Traumatol Arthrosc 2018;26(7):2080–7.
[6] Freedman BR, Gordon JA, Soslowsky LJ. The Achilles tendon: fundamental properties and mechanisms governing healing. Muscles Ligaments Tendons J 2014;4(2):245–55.
[7] Andarawis-Puri N, Flatow EL. Promoting effective tendon healing and remodeling. J Orthop Res 2018;36(12):3115–24.
[8] Bottagisio M, Lovati AB. A review on animal models and treatments for the reconstruction of Achilles and flexor tendons. J Mater Sci Mater Med 2017;28(3):45.
[9] Wang Z, Liu X, Davies MR, Horne D, Kim H, Feeley BT. A mouse model of delayed rotator cuff repair results in persistent muscle atrophy and fatty infiltration. Am J Sports Med 2018;46(12):2981–9.
[10] Hast MW, Zuskov A, Soslowsky LJ. The role of animal models in tendon research. Bone Joint Res 2014;3(6):193–202.
[11] Beason DP, Kuntz AF, Hsu JE, Miller KS, Soslowsky LJ. Development and evaluation of multiple tendon injury models in the mouse. J Biomech 2012;45(8):1550–3 [English].
[12] Zhang K, Hast MW, Izumi S, Usami Y, Shetye S, Akabudike N, et al. Modulating glucose metabolism and lactate synthesis in injured mouse tendons: treatment with dichloroacetate, a lactate synthesis inhibitor, improves tendon healing. Am J Sports Med 2018;46(9):2222–31.
[13] Zhang J, Pan T, Wang JH. Cryotherapy suppresses tendon inflammation in an animal model. J Orthop Translat 2014;2(2):75–81.
[14] Ackerman JE, Loiselle AE. Murine flexor tendon injury and repair surgery. J Vis Exp 2016;115.
[15] Lin D, Alberton P, Caceres MD, Volkmer E, Schieker M, Docheva D. Tenomodulin is essential for prevention of adipocyte accumulation and fibrovascular scar formation during early tendon healing. Cell Death Dis 2017;8(10):e3116.
[16] Wong JK, Alyouha S, Kadler KE, Ferguson MW, McGrouther DA. The cell biology of suturing tendons. Matrix Biol 2010;29(6):525–36 [English].
[17] Wong JK, Cerovac S, Ferguson MW, McGrouther DA. The cellular effect of a single interrupted suture on tendon. J Hand Surg Br 2006;31(4):358–67 [English].
[18] Palmes D, Spiegel HU, Schneider TO, Langer M, Stratmann U, Budny T, et al. Achilles tendon healing: long-term biomechanical effects of postoperative mobilization and immobilization in a new mouse model. J Orthop Res 2002;20(5):939–46 [English].
[19] Zhang K, Asai S, Hast MW, Liu M, Usami Y, Iwamoto M, et al. Tendon mineralization is progressive and associated with deterioration of tendon biomechanical properties, and requires BMP-Smad signaling in the mouse Achilles tendon injury model. Matrix Biol 2016;52-54:315–24 [English].
[20] O'Brien EJ, Shrive NG, Rosvold JM, Thornton GM, Frank CB, Hart DA. Tendon mineralization is accelerated bilaterally and creep of contralateral tendons is increased after unilateral needle injury of murine achilles tendons. J Orthop Res 2013;31(10):1520–8 [English].
[21] Tuzmen C, Verdelis K, Weiss L, Campbell P. Crosstalk between substance P and calcitonin gene-related peptide during heterotopic ossification in murine Achilles tendon. J Orthop Res 2018;36(5):1444–55.
[22] Zimmermann SM, Schwitter LW, Scheyerer MJ, Jentzsch T, Simmen HP, Werner CML. Prevention of heterotopic ossification: an experimental study using a plasma expander in a murine model. BMC Surg 2016;16 [English].
[23] Keller A, Ortiz C, Wagner E, Wagner P, Mococain P. Mini-open tenorrhaphy of acute Achilles tendon ruptures: medium-term follow-up of 100 cases. Am J Sports Med 2014;42(3):731–6.
[24] Ateschrang A, Gratzer C, Weise K. Incidence and effect of calcifications after open-augmented Achilles tendon repair. Arch Orthop Trauma Surg 2008;128(10):1087–92 [English].
[25] Kraus R, Stahl JP, Meyer C, Pavlidis T, Alt V, Horas U, et al. Frequency and effects of intratendinous and peritendinous calcifications after open Achilles tendon repair. Foot Ankle Int 2004;25(11):827–32 [English].
[26] Howell K, Chien C, Bell R, Laudier D, Tufa SF, Keene DR, et al. Novel model of tendon regeneration reveals distinct cell mechanisms underlying regenerative and fibrotic tendon healing. Sci Rep 2017;7:45238.
[27] Bell R, Taub P, Cagle P, Flatow EL, Andarawis-Puri N. Development of a mouse model of supraspinatus tendon insertion site healing. J Orthop Res 2015;33(1):25–32 [English].
[28] Liu X, Laron D, Natsuhara K, Manzano G, Kim HT, Feeley BT. A mouse model of massive rotator cuff tears. J Bone Joint Surg Am 2012;94(7):e41.
[29] Hochstrat E, Muller M, Frank A, Michel P, Hansen U, Raschke MJ, et al. Cryopreservation of tendon tissue using dimethyl sulfoxide combines conserved cell vitality with maintained biomechanical features. PloS One 2019;14(4):e0215595.
[30] Freedman BR, Sarver JJ, Buckley MR, Voleti PB, Soslowsky LJ. Biomechanical and structural response of healing Achilles tendon to fatigue loading following acute injury. J Biomech 2014;47(9):2028–34 [English].
[31] Sahin H, Tholema N, Petersen W, Raschke MJ, Stange R. Impaired biomechanical properties correlate with neoangiogenesis as well as VEGF and MMP-3 expression during rat patellar tendon healing. J Orthop Res 2012;30(12):1952–7.

[32] Lillie RD, Tracy RE, Pizzolato P, Donaldson PT, Reynolds C. Differential staining of collagen types in paraffin sections: a color change in degraded forms. Virchows Arch A Pathol Anat Histol 1980;386(2):153–9.
[33] Mowry RW. Revised method producing improved coloration of acidic polysaccharides with alcian blue 8GX supplied currently. J Histchem Cytochem 196;8:323–4.
[34] Dourte LM, Pathmanathan L, Jawad AF, Iozzo RV, Mienaltowski MJ, Birk DE, et al. Influence of decorin on the mechanical, compositional, and structural properties of the mouse patellar tendon. J Biomech Eng 2012;134(3):031005 [English].
[35] Lujan TJ, Underwood CJ, Jacobs NT, Weiss JA. Contribution of glycosaminoglycans to viscoelastic tensile behavior of human ligament. J Appl Physiol (1985) 2009; 106(2):423–31 [English].
[36] Dourte LM, Kuntz AF, Soslowsky LJ. Twenty-five years of tendon and ligament research. J Orthop Res 2008;26(10):1297–305.
[37] Probst A, Palmes D, Freise H, Langer M, Joist A, Spiegel HU. A new clamping technique for biomechanical testing of tendons in small animals. J Invest Surg 2000; 13(6):313–8 [English].
[38] Hillin CD, Fryhofer GW, Freedman BR, Choi DS, Weiss SN, Huegel J, et al. Effects of immobilization angle on tendon healing after achilles rupture in a rat model. J Orthop Res 2019;37(3):562–73. https://doi.org/10.1002/jor.24241.
[39] Freedman BR, Rodriguez AB, Leiphart RJ, Newton JB, Ban E, Sarver JJ, et al. Dynamic loading and tendon healing affect multiscale tendon properties and ECM stress transmission. Sci Rep 2018;8(1):10854.
[40] Wieskotter B, Herbort M, Langer M, Raschke MJ, Wahnert D. The impact of different peripheral suture techniques on the biomechanical stability in flexor tendon repair. Arch Orthop Trauma Surg 2018;138(1):139–45.
[41] De la Fuente C, Pena y Lillo R, Carreno G, Marambio H. Prospective randomized clinical trial of aggressive rehabilitation after acute Achilles tendon ruptures repaired with Dresden technique. Foot (Edinb) 2016;26:15–22 [English].
[42] Huang J, Wang C, Ma X, Wang X, Zhang C, Chen L. Rehabilitation regimen after surgical treatment of acute Achilles tendon ruptures: a systematic review with meta-analysis. Am J Sports Med 2015;43(4):1008–16 [English].
[43] O'Brien EJ, Frank CB, Shrive NG, Hallgrimsson B, Hart DA. Heterotopic mineralization (ossification or calcification) in tendinopathy or following surgical tendon trauma. Int J Exp Pathol 2012;93(5):319–31 [English].
[44] Wunderli SL, Widmer J, Amrein N, Foolen J, Silvan U, Leupin O, et al. Minimal mechanical load and tissue culture conditions preserve native cell phenotype and morphology in tendon-a novel ex vivo mouse explant model. J Orthop Res 2018; 36(5):1383–90.
[45] Shi Y, Fu Y, Tong W, Geng Y, Lui PP, Tang T, et al. Uniaxial mechanical tension promoted osteogenic differentiation of rat tendon-derived stem cells (rTDSCs) via the Wnt5a-RhoA pathway. J Cell Biochem 2012;113(10):3133–42 [English].
[46] Qin S, Wang W, Liu Z, Hua X, Fu S, Dong F, et al. Fibrochondrogenic differentiation potential of tendon-derived stem/progenitor cells from human patellar tendon. J Orthopaed Translat 2019. In press, https://doi.org/10.1016/j.jot.2019.08.006.
[47] Ackerman JE, Bah I, Jonason JH, Buckley MR, Loiselle AE. Aging does not alter tendon mechanical properties during homeostasis, but does impair flexor tendon healing. J Orthop Res 2017;35(12):2716–24.
[48] Lui PP, Cheuk YC, Lee YW, Chan KM. Ectopic chondro-ossification and erroneous extracellular matrix deposition in a tendon window injury model. J Orthop Res 2012;30(1):37–46 [English].
[49] Liu Y, Suen CW, Zhang JF, Li G. Current concepts on tenogenic differentiation and clinical applications. J Orthop Translat 2017;9:28–42.
[50] Snedeker JG, Foolen J. Tendon injury and repair - a perspective on the basic mechanisms of tendon disease and future clinical therapy. Acta Biomater 2017;63: 18–36.